B3

GANIL

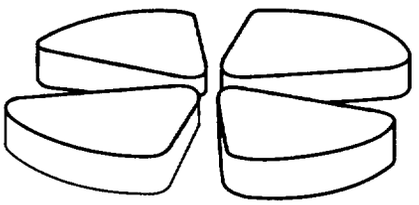

Neutron multiplicity distributions for 200 MeV proton-, deuteron- and ^{4}He-induced spallation reactions on thick Pb targets

B. Lott*[a], F. Cnigniet[a], J. Galin[a], F. Goldenbaum[a], D. Hilscher[b], A. Liénard[a], A. Péghaire[a], Y. Périer[a], X. Qian[a]

[a]GANIL (IN2P3-CNRS, DSM-CEA), BP 5027, F-14076 Caen Cedex 5, France

[b]Hahn-Meitner-Institut Berlin, Glienickerstr. 100, D-14109 Berlin, Germany

SIN9749

GANIL P 97 37

Neutron multiplicity distributions for 200 MeV proton-, deuteron- and ^{4}He-induced spallation reactions on thick Pb targets

B. Lott*[a], F. Cnigniet[a], J. Galin[a], F. Goldenbaum[a], D. Hilscher[b], A. Liénard[a], A. Péghaire[a], Y. Périer[a], X. Qian[a]

[a]GANIL (IN2P3-CNRS, DSM-CEA), BP 5027, F-14076 Caen Cedex 5, France

[b]Hahn-Meitner-Institut Berlin, Glienickerstr. 100, D-14109 Berlin, Germany

Inclusive neutron multiplicity distributions associated with 197 MeV proton-, 188 MeV deuteron- and 214 MeV ^{4}He-induced spallation reactions on thick (l=2-25 cm) Pb targets are presented, together with distributions associated with nuclear-reaction events. The mean neutron multiplicity per incident particle, <n/p>, which is a crucial parameter for applications on accelerator-driven neutron sources, has been obtained for various conditions. For the thickest targets used in this work, all distribution characteristics are found nearly identical for reactions induced by protons and deuterons.

1. Introduction

The recent blossoming of projects on intense neutron sources based upon spallation reactions induced by energetic light projectiles has prompted a renewal of interest in related data, both with thin or thick targets. Of chief importance in this context is the average energy spent per neutron produced, $<E_{part}/n>$, which governs the efficiency and in turn the operating cost of the proposed facilities. Although the optimal energy for which $<E_{part}/n>$ is a minimum appears to lie around 1 GeV for protons, justifying the considerable experimental effort in this energy range, the need of new data at lower energy has grown as well, for two main reasons. On the one hand, these data may give insight into the internuclear part of the cascade, i.e. the neutron production induced by secondary particles of lower energy in the thick target material. On the other hand, using a 200 or 300 MeV light-particle beam can prove interesting from the practical standpoint as the higher reachable beam intensity may compensate for a less favorable $<E_{part}/n>$. The data presently available with thick targets in the above E_{part} range are rather scarce [1–5] and most often concern only a limited range in neutron energy because of high detection thresholds. These considerations have motivated the present work, in which the neutron multiplicity *distributions* measured with Pb targets of different thicknesses (l=2 to 25 cm) are presented for reactions induced by 197 MeV p, 188 MeV d and 214 MeV ^{4}He. The comparison between data obtained with the two former projectiles can shed light on the role played by deuteron-breakup reactions, which are expected to enhance significantly the neutron production. This expected enhancement has led several projects [6,7] of intense neutron source facilities to adopt d rather than p as the projectile.

The experimental method employed in the present work makes use of a segmented calorimetric 4π detector, ORION, to measure the neutrons. This "calorimetric" (also called "moderator") method has been largely used to study the neutron emission in heavy-ion collisions [8], or in light-particles spallation reactions with thin targets [9,10] and more recently with thick targets [11,12]. The advantages offered by this method are multifold: in addition to supplying the total (inclusive) neutron multiplicity distribution, the detector provides the distribution associated with nuclear reactions, the reaction probability P_{reac} and a rough determination of the angular distributions of the detected neutrons thanks to its segmented design. A definite asset of the

[1]Cooresponding author, electronic mail address: LOTT@GANAC4.IN2P3.FR

method comes from the virtually non-existent energy threshold of ORION, which is of primary importance in detecting neutrons produced in thick targets, associated with a very soft energy spectrum.

2. Experimental method

As very low-intensity beams (I < 1000 particles/s) are sufficient in this method because of the large detection efficiency offered by ORION, use was made of secondary beams produced at the Grand Accélérateur d'Ions Lourds (GANIL) by fragmentation of an intense (2.10^{13} p/s) 95 A.MeV ^{13}C beam onto a 9 mm-thick C target. The particles were sorted via an analyzing spectrometer and tagged with a 1 mm-thick plastic scintillator detector positioned 57 cm upstream of the target in ORION's reaction chamber. In addition to triggering the neutron counting, this detector allowed for a full identification of the traversing particles by providing an energy-loss information and the stop signal of a time of flight measurement with respect to the cyclotron radio frequency. For the proton measurements, a thin wedge acting as an achromatic degrader was inserted between the two dipoles of the spectrometer, which were adjusted to slightly different magnetic rigidities so that only protons could pass through. The total light-particle rate did not exceed 1000 particles/s to limit the probability of pile-up events to less than 5% during the neutron counting. The pile-up events have been rejected with 100% efficiency in the off-line analysis by demanding that no particle traversed the plastic detector during the neutron counting. The lead targets were 12 cm in diameter with thicknesses varying between 2 and 25 cm. The setup is schematically depicted in Fig. 1.

The 4π neutron counter, ORION, consists of five sectors filled with Gd-loaded (0.3% in weight) liquid scintillator representing a total volume of 4 m^3. The light created within ORION is collected by means of 30 phototubes (6 per sector). The principle of operation of such a detector is the following. The neutrons are initially slowed down by scattering off hydrogen and carbon nuclei making up the solvent. The total recoil energy of these nuclei together with the energy of γ-rays emitted in the reaction are converted into light by the scintillator, leading to what is referred to as the "prompt" response. This response was exploited in the present experiment to signify the occurrence of a nuclear reaction in the target, provided that more than 2 MeVee of light is measured with ORION. Although this condition is fulfilled for virtually all inelastic reactions taking place in thin targets, some events associated with low energy dissipation may not be labeled as such in the case of thick targets made of heavy material because of the strong absorption of γ-rays. This effect is discussed further below.

During the moderation stage, some neutrons either escape or are captured in nuclear reactions with C nuclei. The remaining neutrons, by far the majority at low neutron energy, are eventually slowed down to thermal energies and then, on a time scale of a few μs, undergo radiative capture reactions with Gd nuclei, resulting in the emission of several γ-rays. The light produced in the detection of these γ-rays corresponds to the "delayed" response, which was measured in the present case over a 50 μs counting time. The correlated background was measured during a second counting gate delayed by 400 μs with respect to the first one, and subtracted off-line. The average multiplicity corresponding to this background amounted to 0.55. More details on the method can be found in ref [11–13].

For the sake of illustration, Fig.2 displays the experimental capture time distribution obtained with neutrons emitted from a Cf source together with results of the Monte-Carlo simulation described below, assuming a concentration of 0.3% wt of Gd (dashed curve). The capture time distribution can be fitted with a functional of the following form [13] (solid curve):

$$\frac{dP}{dt} = \frac{\beta\alpha^2}{(\beta-\alpha)^2}(e^{-\alpha t}((\beta-\alpha)t-1)+e^{-\beta t}) \quad (1)$$

where α and β depend on the H and Gd concentrations in the liquid respectively. For the liquid used in ORION, the fitted values are α=0.36μs^{-1} and β=0.086μs^{-1}.

The efficiency to neutrons was continuously monitored during the experiment with a Cf neu-

tron source sitting inside the reaction chamber close to the target. An efficiency of 79.6% to neutrons emitted in the spontaneous fission of Cf, of mean energy 2.1 MeV was obtained with a threshold of 2 MeVee (averaged over the five sectors) on the light output. The ORION efficiency is strongly dependent on the neutron energy as illustrated in Fig.3, which displays the efficiency curve for ORION's delayed response calculated by means of the DENIS [14] Monte-Carlo simulation code. The very good reliability of such theoretical predictions has been checked recently, when the efficiencies measured [15] in a calibration experiment with neutron beams at several energies provided by the Louvain-La-Neuve facility were reproduced by the DENIS simulation within a few per cent.

For target thicknesses shorter than the range of the impinging particles (r=4.7cm, 2.7cm and 0.45cm for 197 Mev p, 188 MeV d and 214 MeV ^{4}He, respectively), traversing beam particles scattered off-axis in the target could interact with the forward wall of the reaction chamber. Thanks to the time difference in the prompt signal issued by ORION, a partial correction could be applied to the affected distributions, the associated uncertainty translating into larger error bars for the corresponding data.

The mean values given in the following are corrected assuming a constant efficiency equal to that found for the Cf neutrons, although high-energy neutrons may be produced in the reactions. However, this approximation appears quite justified in view of the large target thicknesses and the moderate energy of the impinging light particles, both factors leading to a soft energy spectrum of the "leaking" neutrons. It must be emphasized that this assumption was also employed in all previous moderator measurements of mean multiplicities.

3. Results

The distributions obtained with 197 MeV p, 188 MeV d and 214 MeV ^{4}He are compared in Fig. 4 for the thickest targets. Histograms depict inclusive distributions, whereas symbols correspond to distributions obtained for reaction events (selected by requesting the ORION prompt signal in coincidence with the incident particles). The latter distributions can be fitted very well with Gaussians while the no-reaction events are associated essentially with the background multiplicity distribution. As pointed out above, the latter follows a Poisson distribution of mean 0.55. The distributions associated with 197 MeV p and 188 MeV d are surprisingly similar, the inclusive ones as well as those obtained for reaction events. For instance, the means of the inclusive distributions for the thickest targets used are found to be the same within the error bars: $<n/p>=1.440\pm.005$ and $<n/d>=1.43\pm.02$ (corrected with a constant efficiency of 79.6%). In comparison, reactions involving α-particles are found much less suitable for neutron production. The parameters measured for the different projectiles for l=25cm (l=20cm for d) are given in Table 1.

A more detailed comparison between the mean neutron multiplicities obtained with p and d is displayed in Fig. 5 as a function of the target thickness, for the inclusive distributions (lower panel) and those associated with reaction events, $<n/part>_{reac}$ (upper panel). The rise of the neutron multiplicity with the target thickness results from two effects: an increasing reaction probability, P_{reac}, and the production of additional neutrons via secondary reactions taking place within the target material. The former effect underlies the steep increase in the observed multiplicity for thicknesses shorter than the particle range. For protons, P_{reac} increases from $11\pm1\%$ to $15.7\pm.1\%$ between l=2cm and 5cm and remains virtually constant for larger thicknesses. For deuterons, one obtains $P_{reac}=15\pm1\%$ for l=2cm and $P_{reac}=16.5\pm0.2\%$ for $l\geq3$ cm. For ^{4}He, the reaction probability is only $3.20\pm0.08\%$, due to the very short range of these particles in Pb. P_{reac} reads:

$$P_{\rm reac} = 1 - \exp(-\int_{V_B}^{E} \rho\sigma_R(E)(-\frac{dE}{dx})^{-1}dE) \quad (2)$$

with $\sigma_R(E)$, V_B, ρ and $(-\frac{dE}{dx})$ being the energy-dependent reaction cross section, Coulomb barrier, the density of target nuclei, and the electronic stopping power, respectively. Using the

stopping powers from Ziegler [16] and the cross sections taken from ref. [17,18], one finds the calculated probabilities listed in Table 1. The relative magnitudes of the observed reaction probabilities are accounted for by the calculations, but are found about 30% lower than the calculated ones for p and d. (A similar effect, although less pronounced, was observed [12] at higher bombarding energy). This discrepancy may stem from the loss of some reaction events associated with low neutron multiplicities, which would not give rise to a prompt signal in ORION large enough to overcome the electronic threshold. This explanation is supported by the absence of any low-multiplicity peak in the present distributions associated with reaction events, while corresponding distributions measured [9,12] with thinner targets did exhibit such peaks. In studies involving thin targets, these events are recorded thanks to the detection of the associated γ-rays, which are strongly absorbed inside the thick Pb targets employed in the present case. The values of $<n/part>_{reac}$ given above may thus be significantly overestimated. It must however be stressed that the inclusive distributions, which are the relevant ones as far as spallation neutron sources are concerned, are not affected by this shortcoming of the method.

The increase in <n/part > observed in Fig. 5 for target thicknesses larger than the particle ranges stems solely from the secondary reactions taking place within the target material. The multiplication factor observed between l=5cm and l=20cm is very moderate, equal to 1.06 and 1.10 for p and d,respectively. The somewhat larger factor found for d can be tentatively ascribed to breakup reactions that give rise to a larger flux of high-energy neutrons at forward angles susceptible to multiply in the medium. However, these reactions occur for only a few percent of the events, as confirmed by a theoretical estimation [21] of the corresponding breakup cross-section, found to be at most 1 b for E/A<100MeV.

The <n/p> values can be compared to the predictions of empirical formulae, like the "E-120" rule [19], established for l=1m and d=20cm Pb targets and p energies between 0.5 GeV and 1.5 GeV: $<n/p>=0.1(E_{GeV} - .12)(A+20)$, where A is the atomic mass of the target medium. The above formula yields <n/p>=1.75. The 20% discrepancy found with respect to the experimental data is remarkably low in view of the crudeness of the "E-120" formula, and considering also the difference in target geometry. More sophisticated calculations performed with the computer code LAHET [20] reproduce the experimental <n/d> value for l=25cm but underestimate this multiplicity for smaller thicknesses (by about 20% at l=5cm), which is indicative of an overestimation of the internuclear neutron multiplication, possibly due to an overestimated deuteron breakup probability.

Some insight into the detected-neutron angular distributions can be gained thanks to ORION's segmented design. Fig.6a displays the relative multiplicities, Mn, recorded by the different ORION sectors (see Fig. 1), measured with p and d for l=20cm. Again, it is interesting to note that the angular distributions exhibited by neutrons produced in p- and d-induced reactions are very similar, although the bombarding velocities are quite different (β_p=0.56, β_d=0.41). The slight excess observed for d in the most forward sector is presumably due to breakup neutrons. Fig.6b shows the same multiplicities as Fig.6a but normalized to the corresponding multiplicities obtained for Cf neutrons, which serve as a benchmark for isotropic emission (in this case, the source was placed on the beam axis in contact with the thick target so that the distortion of the angular distribution due to neutrons scattering off target nuclei was partly accounted for). The neutron angular distributions are slightly forward peaked, manifesting the presence of a direct-neutron component, but more importantly they reveal a strong contribution of isotropically emitted neutrons, comprising low-energy evaporated as well as Pb-moderated neutrons. The latter observation justifies to a large extent the use of a constant efficiency determined with 2.1 MeV Cf neutrons in the correction procedure. It is worth mentioning that the distribution of prompt light collected in ORION which reflects the neutron energy is very soft albeit exhibiting at forward angle a harder component corresponding to direct neutrons. Surprisingly, the distributions associated

with p and d are again found nearly identical, despite the difference in bombarding energy per nucleon.

4. Conclusion

For the first time, neutron multiplicity distributions have been measured for p, d and α particles bombarding thick Pb targets in the 200 MeV energy range. All distribution characteristics are found very similar for p and d at the same total bombarding energy, as already observed at higher energy [11]. This observation is indicative of the marginal role played by deuteron breakup reactions in the neutron production process. The observed average neutron multiplicities agree within 20% with systematics established for higher bombarding energies. Most of the available energy is dissipated in the form of electronic energy loss in the target material, translating into a $<E_p/n>$ ratio of 139 MeV/n at 200 MeV to be compared to $<E_p/n> \simeq 50$ MeV/n at the "optimum energy" of 1 GeV [11], for example. The poor efficiency of the neutron production with either p or d projectiles around 200 MeV makes the choice of this energy *a priori* quite unsuitable for intense neutron sources. However, other factors related to the feasibility of high-intensity and high-energy accelerators or to radiation safety are also relevant to this choice and may favor a lower energy than the "optimum energy" of 1 GeV.

5. Acknowledgments

The authors would like to thank D. Ridikas for performing simulation calculations with the LAHET computer code. It is also a pleasure to thank U. Jahnke for fruitful discussions.

REFERENCES

1. M. Berkovitch et al., *Phys. Rev.* **119** (1960) 412.
2. J. W. Wachter et al., *Phys. Rev.* **161** (1967) 971.
3. S. Cierjacks et al., Proc. IV ICANS Meeting at KEK, Oct. 20-24, 1980.
4. M. A. Lone et al., *Nucl. Instr. and Meth.* **214** (1983) 333.
5. S. Cierjacks et al., *Phys. Rev.* **C36** (1987) 1976.
6. D. Ridikas et W. Mittig, Ganil preprint P97-19.
7. Concept for Advanced Exotic Beam Facility Based on Atlas, Argonne National Laboratory (February 1995).
8. J. Galin and U. Jahnke, *J. Phys. G: Nucl. Part. Phys.* **20** (1994) 1105 and references therein.
9. L. Pienkowski et al., *Phys. Lett.* **B336** (1994) 147.
10. F. Goldenbaum et al., *Phys. Rev. Lett.* **77** (1996) 1230.
11. L. Pienkowski et al., *Phys. Rev.***C 56** (1997) 1909.
12. D. Hilscher et al., *Nucl. Instr. and Meth. A*, this issue.
13. U. Jahnke et al., *Lecture Notes in Physics*, (Springer Verlag Ed., Berlin) 178 (1983).
14. J. Poitou and C. Signarbieux, *Nucl. Instr. and Meth.* **114** (1974) 113.
15. Y. Périer, to be published.
16. H.H. Andersen and J.F. Ziegler in *The Stopping and Ranges of Ions in Matter*, (Pergamon Press, New York, Toronto, Oxford, Sydney, Frankfurt, Paris, 1977).
17. A. Fasso, K. Goebel, M. Höfert, J. Ranft, G. Stevenson, **Landolt Börnstein**, *New Series 1/11* (1990), ed. H. Schopper, p.71.
18. R.F. Carlson, *Nucl. Data Tables* **63** (1996) 93 and references therein.
19. J. S. Fraser et al., *Phys. Can.* **21** (1966) 17.
20. R.E. Prael and H. Lichtenstein, Los Alamos National Laboratory Report LA-UR-89-3014, (September 1989).
21. C.A. Bertulani and G. Baur, *Nucl. Phys.* **A480** (1988) 615.

Proj.	E (MeV)	range (cm)	P_{reac} meas.(%)	P_{reac} calc.(%)	<n/p>	$<n/p>_{reac}$
p	197	4.7	15.7	21.1	1.440±.005	7.28±0.02
d	188	2.7	16.5	22.5	1.43±.02	7.3±.05
α	214	0.45	3.2	3.5	.296±.007	8.10±.15

Table 1
Comparison of the results obtained for a l=25cm (l=20cm for d) Pb target

Figure captions

Figure 1. Schematic view of the experimental setup.

Figure 2. Experimental capture time distribution (histogram) compared with that calculated with the simulation code DENIS (dashed curve). The solid curve corresponds to the fit with the function given in eq. (1).

Figure 3. Efficiency of the ORION detector as a function of the neutron energy as calculated with DENIS [14].

Figure 4. Neutron multiplicity distributions obtained inclusively (histograms) and in coincidence with a prompt signal in ORION (symbols), as measured, for the three projectiles used in the present experiment.

Figure 5. Mean neutron multiplicities (corrected for background and efficiency) of the inclusive distributions (lower panel) and those associated with reaction events as defined in the text (upper panel), for l=20cm. The solid and open arrows indicate the ranges in lead for 197 MeV p and 188 MeV d, respectively.

Figure 6.a) Partial neutron multiplicities, Mn, obtained with the different ORION sectors for a l=20 cm Pb target. The latter was located at the center of sector 3. b) Same as a) but the partial multiplicities have been normalized to those obtained with the Cf source, which was placed on the beam axis against the target entrance plane.

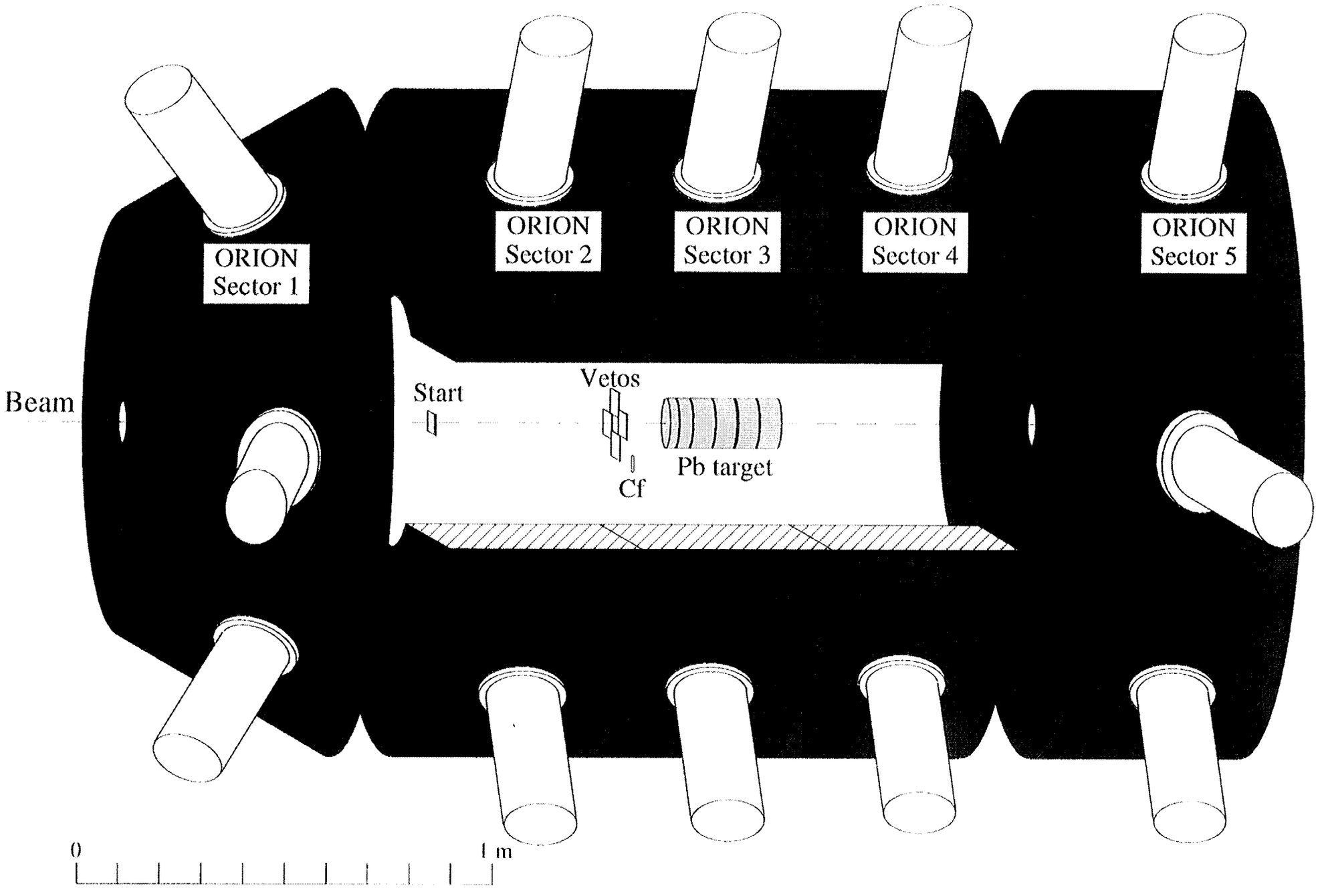
ORION
Sector 1
ORION
Sector 2
ORION
Sector 3
ORION
Sector 4
ORION
Sector 5
Beam
Start
Vetos
Cf
Pb target
0
1 m

Fig. 1

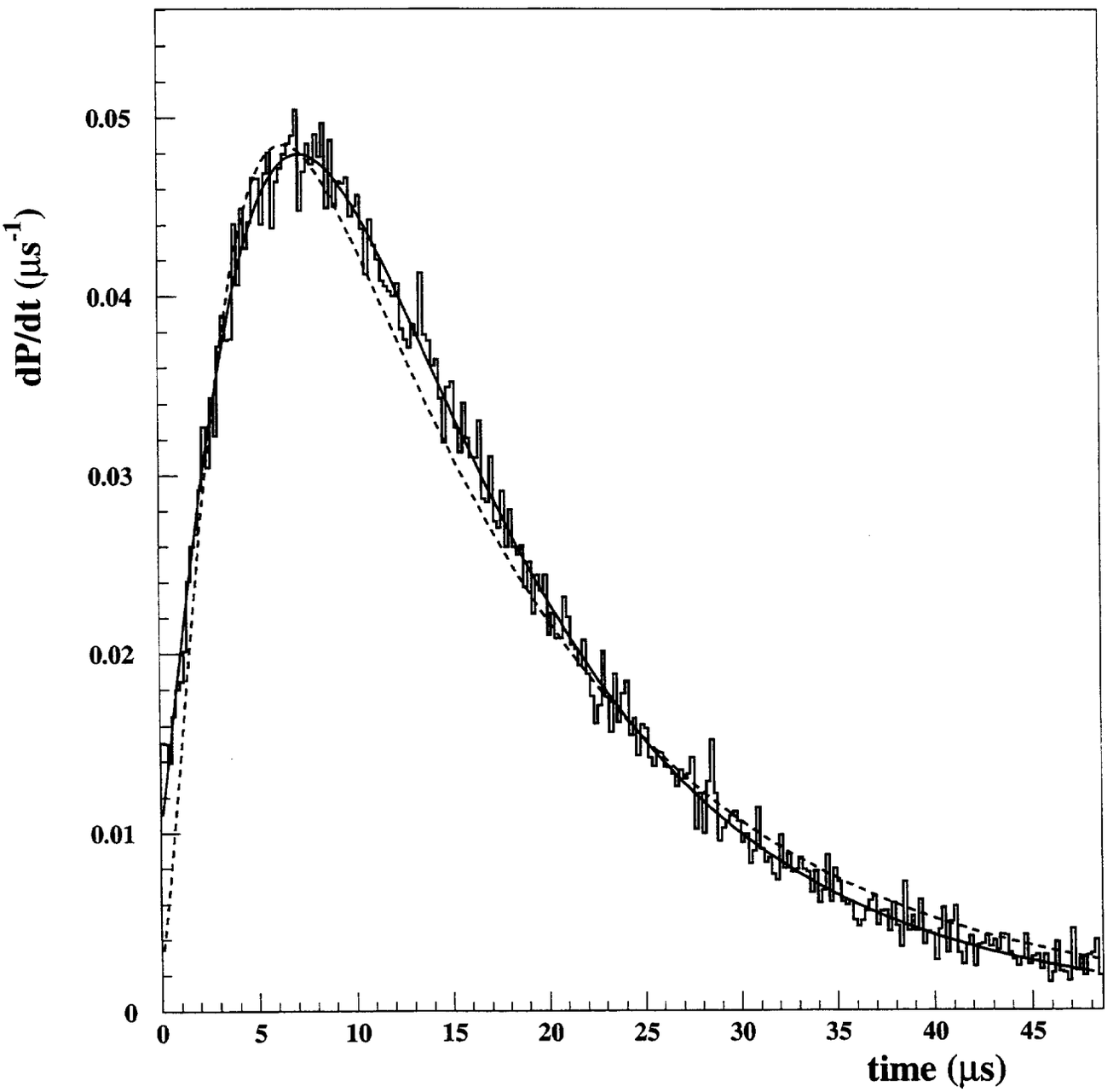

Fig. 2

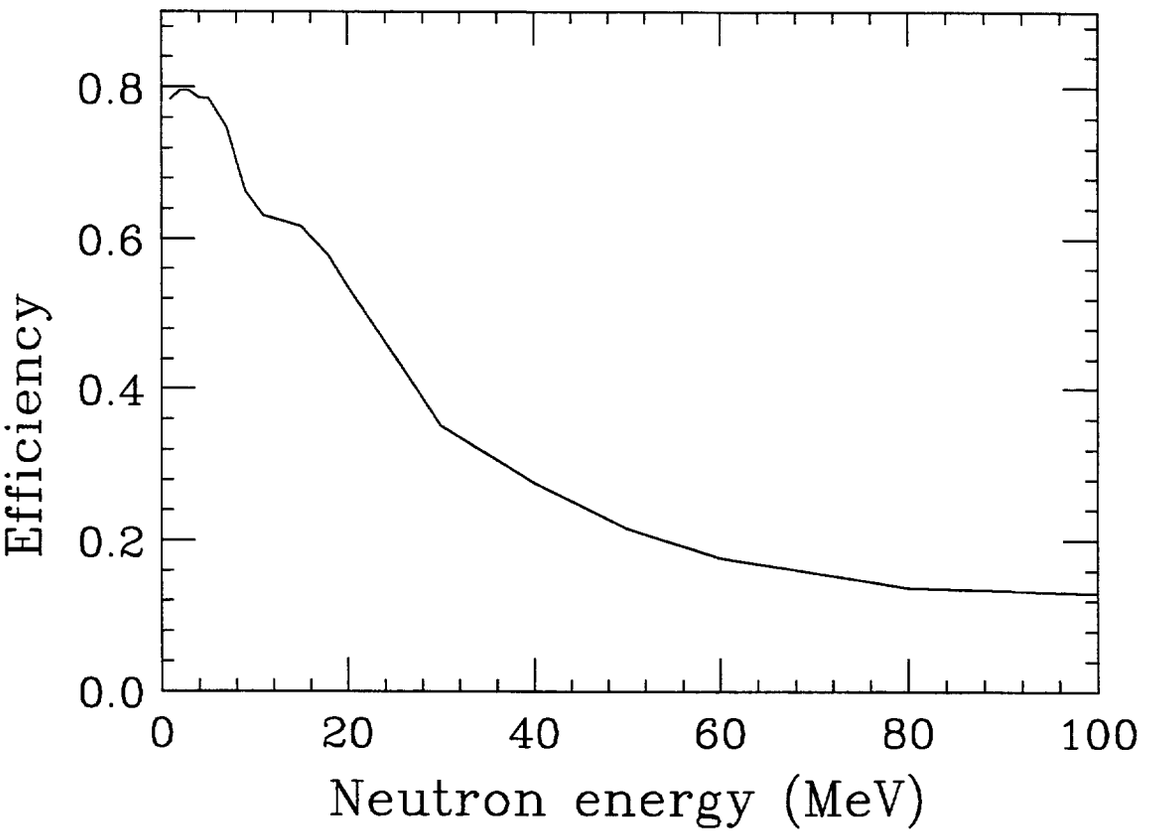

Fig. 3

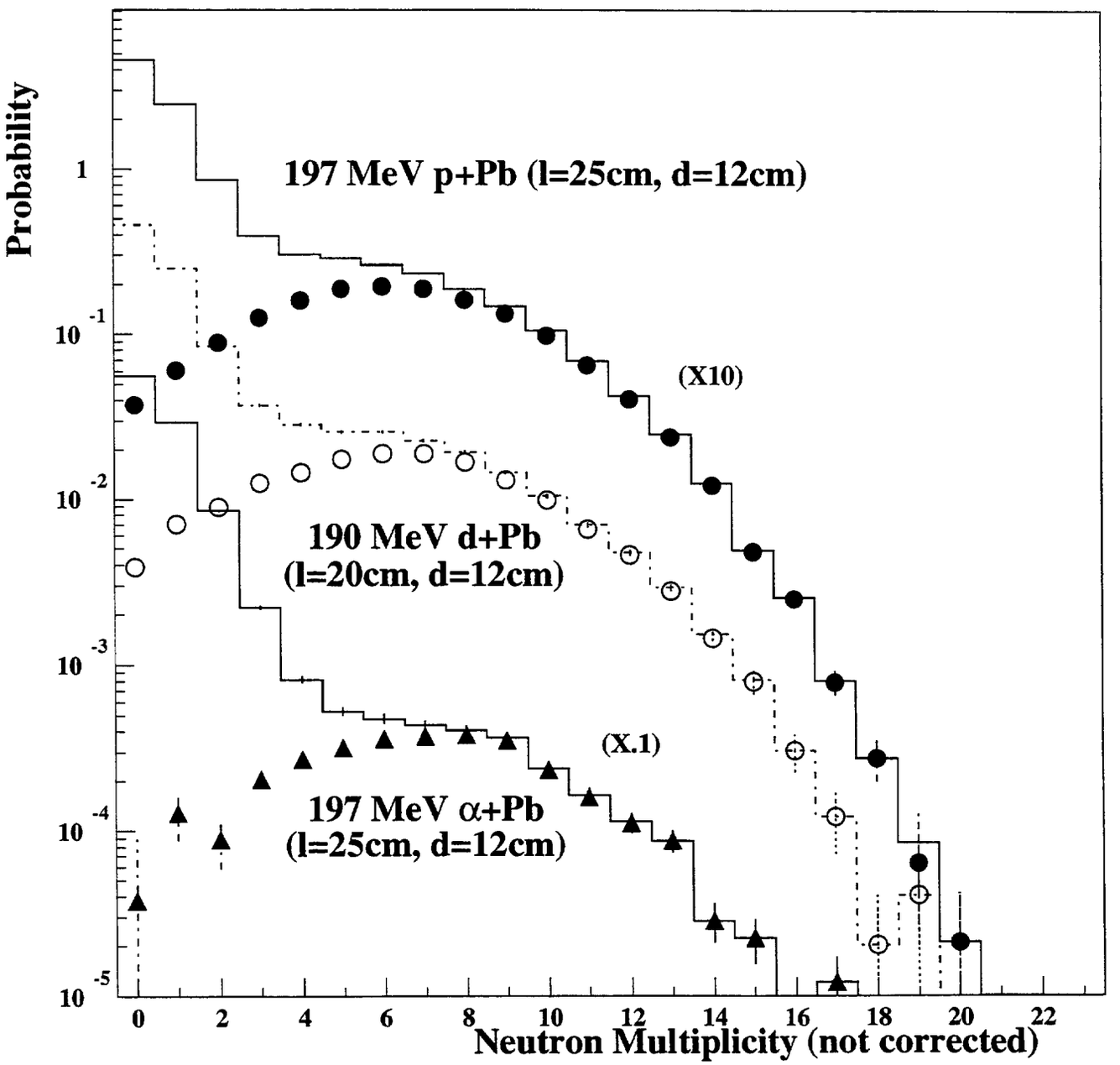
Probability
1
10^-1
10^-2
10^-3
10^-4
10^-5
197 MeV p+Pb (l=25cm, d=12cm)
(X10)
190 MeV d+Pb
(l=20cm, d=12cm)
(X.1)
197 MeV α+Pb
(l=25cm, d=12cm)
0
2
4
6
8
10
12
14
16
18
20
22
Neutron Multiplicity (not corrected)

Fig. 4

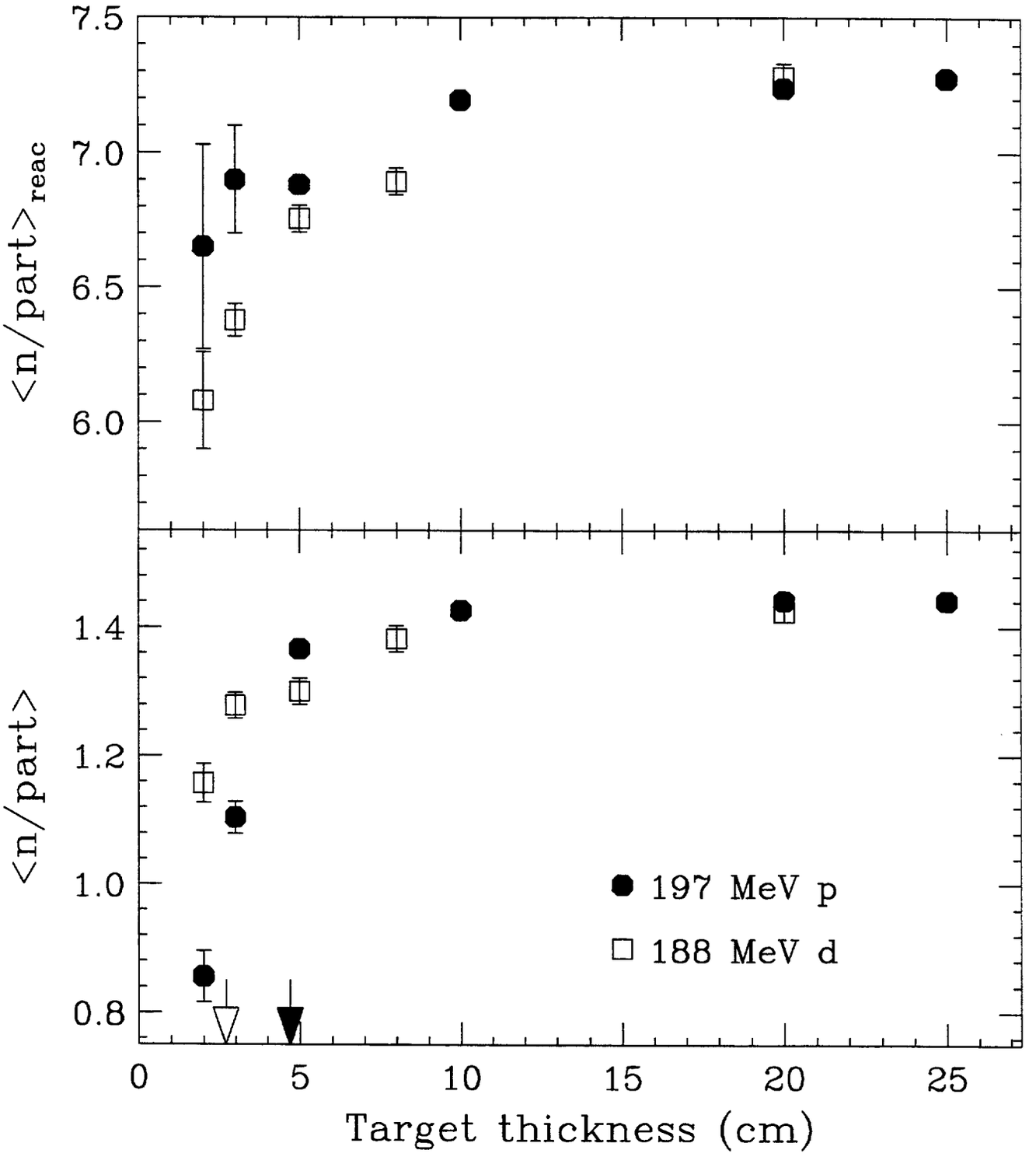
7.5
7.0
6.5
6.0
<n/part>reac
1.4
1.2
1.0
0.8
<n/part>
197 MeV p
188 MeV d
0
5
10
15
20
25
Target thickness (cm)

Fig. 5

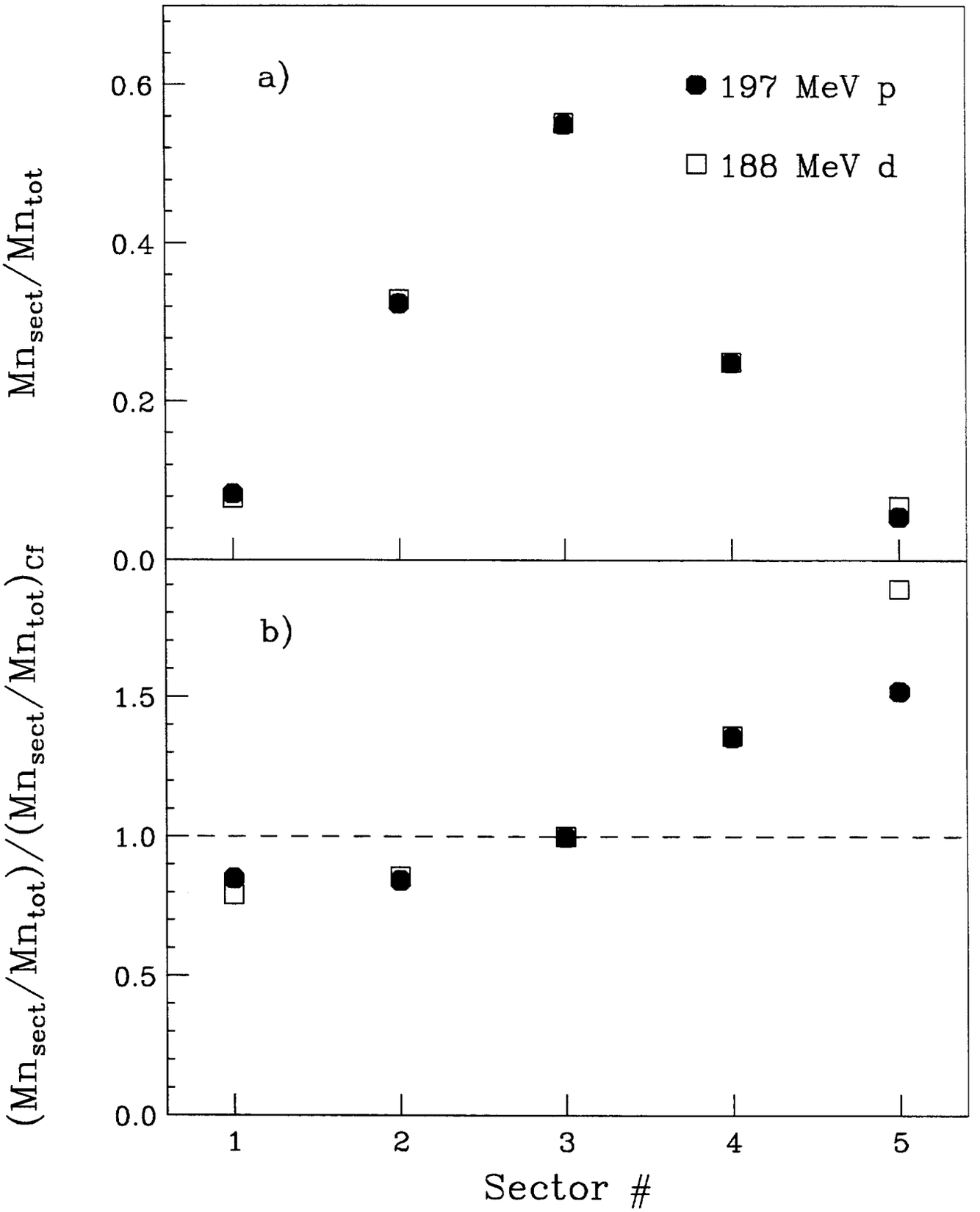
a)
197 MeV p
188 MeV d
0.6
0.4
0.2
0.0
Mn_{sect}/Mn_{tot}
b)
1.5
1.0
0.5
0.0
$(Mn_{sect}/Mn_{tot})/(Mn_{sect}/Mn_{tot})_{CF}$
1
2
3
4
5
Sector #

Fig. 6